Springer

KSME

Journal of Mechanical Science and Technology 26 (8) (2012) 2451~2458
www.springerlink.com/content/1738-494x
DOI 10.1007/s12206-012-0627-9

An analytical model to investigate skidding in rolling element bearings during acceleration †

Wenbing Tu[1], Yimin Shao[1,*] and Chris K. Mechefske[2]

[1]*State Key Laboratory of Mechanical Transmission, Chongqing University, Chongqing 400030, China*
[2]*Department of Mechanical and Materials Engineering, Queen's University, K7L 3N6 ,Canada*

(Manuscript Received July 29, 2011; Revised February 26, 2012; Accepted March 28, 2012)

Abstract

Skidding, which occurs in rolling element bearings during shaft rotational acceleration, causes wear and incipient failure. This paper presents an analytical model to investigate skidding during rolling element bearing acceleration, taking account of the contact force and friction force between the rolling elements and the races and the cage, gravity, and the centrifugal force of the rolling elements. The Hertzian contact theory is applied to calculate the non-linear contact force. The Coulomb friction law is used to calculate the friction force. All forces above are included in force equilibrium equations to derive the non-linear governing equations of the bearing during acceleration, and are solved using a fourth-order Runge-Kutta algorithm with fixed time step. The proposed model is verified by comparison to other published results and with experimental results. The proposed model can be used to investigate skidding in rolling element bearings during acceleration and the transient motion behavior of rolling elements, and it will lay the theoretical foundations for eliminating skidding in rolling element bearings.

Keywords: Rolling element bearing; Skidding; Bearing acceleration; Analytical model

1. Introduction

Rolling element bearings, which are of great importance in numerous rotating machinery systems, often operate in non-steady state conditions when the bearing is supporting an accelerating process. During these processes, the speed of the rolling element bearing will be increased in a short time and skidding occurs when the friction between rolling elements and races is inadequate to overcome cage drag, rolling resistance, gravity, and acceleration resistance. Skidding causes surface wear in the contact area and will reduce the reliability and life of the rolling element bearing.

Many researchers have already studied the skidding behavior of rolling element bearings since 1960s. Numerous analytical and numerical models have been developed. Jones [1, 2] developed the first mathematical model to analyze the motion of rolling elements in ball bearings based on raceway control hypothesis. According to the hypothesis, each rolling element rolls relative to the controlling raceway and also rolls and spins with respect to the non-controlling raceway. Harris [3, 4] pointed out that the raceway control hypothesis was inadequate as a mathematical model because no provision was made for balancing the totality of friction forces and moments acting on each rolling element. Then he developed an analytical model for axially loaded angular contact ball bearing without using the raceway control hypothesis, and the model was more closely approximated the experiment data. Also, Harris [5] proposed an analytical model to predict skidding in high speed roller bearings, taking account of contact force and friction force between roller and races, fluid pressure force and centrifugal force of the roller. The analytical model can be used to determine the extent of skidding and the effectiveness of various means employed to eliminate skidding. Above studies are mainly based on quasi-static analysis techniques with steady state force and moment balances. To understand dynamic skidding behavior of rolling element bearing, it is necessary to develop dynamic models. The first dynamic model for ball bearing was developed by Walters [6], which was concerned with the dynamics of the separator and a constrained ball motion. However, the constrained ball motion assumption will not hold under dynamic conditions [7]. Hence, the formulation cannot be used for investigating skid and other transient phenomenon in ball bearings. Gupta [7] formulated the generalized differential equations of motion for a ball in a thrust loaded angular contact bearing. The motion was considered with six degrees of freedom and the equations may be

*Corresponding author. Tel.: +86 (0)2365112520, Fax.: +86 (0)2365106195
E-mail address: ymshao@cqu.edu.cn
† Recommended by Associate Editor Ohseop Song

integrated with an arbitrary traction-slip relationship. The model did not take the effect of the cage into account. However, the rolling elements will contact with the cage closely during bearing acceleration. Hence, the model cannot be applied to study skidding of rolling element bearing during acceleration.

Recently, Liao et al. [10] investigated the skidding behavior of high speed angular contact ball bearing under radial and axial loads using quasi-static analysis technique. Through the geometric analysis of a ball bearing and the force balance, the normal forces and the contact angle can be obtained. Using the empirical criterion proposed by Hirano [9], the conditions for the proper choice of the total deformations in two directions can be identified in order to avoid bearing skidding. Selvaraj and Marappan [11] developed a test rig to investigate the effect of operating parameters, such as shaft speed, radial load, viscosity of lubricating oil, number of rollers and temperature, on cage slip in cylindrical roller bearing. Laniado-Jacome et al. [13] presented a numerical model of a roller bearing for mechanical event simulations, which was developed with finite element method, to study sliding between the rollers and the races. Jain and Hunt [14] presented a dynamic model formulation, including centrifugal and gyroscopic effects, to investigate the skidding characteristics of angular contact ball bearings for axial as well as combined axial and radial loading conditions. The forces acting on the rolling elements were obtained by quasi-static analysis and the model neglected the inertia of the cage which had an important effect on the cage speed, especially for the time-varying operating conditions.

According to the above analysis, it can be seen that most of previous studies on skidding of rolling element bearings were based on quasi-static models which consist of a set of nonlinear algebraic equations. These models predict the average forces and moments acting on the rolling elements and cage and cannot be used to predict transient effects or time-varying operating conditions. Even though the dynamic models related to the rolling element bearing skidding, they are only considered with the differential equations of motion of rolling elements or with constrained motion, which are approximately true to steady operating conditions. In the process of steady motion of rolling element bearings, the interaction between rolling elements and races is negligible, and the resultant force and resultant moment will be equal to zero. However, if the bearing is involved in an accelerating process, the interaction between rolling elements and races is considerable and the resultant force and resultant moment will drive rolling elements to accelerate. The existing models cannot be applied to investigate skidding in rolling element bearings during acceleration. Rolling element bearings often operate under acceleration and therefore, an accurate model to investigate skidding in rolling element bearings during acceleration is important and urgent.

The primary objective of this paper is to build a dynamic model to investigate skidding in rolling element bearings during acceleration, concerned with the dynamics of inner race, rolling elements and the cage, taking account of the contact force and friction force between rolling elements and races and the cage, gravity, and the centrifugal force of each rolling element. The differential equations of motion of the inner race, the rolling elements and the cage in the bearing are formulated to derive the non-linear governing equations of bearings during acceleration. These equations are then solved using a fourth-order Runge-Kutta algorithm with fixed time step. Constant inner race speed is input into the model and cage speeds are calculated from the model at various radial loads. The model validity is proven by the comparison of our results to those of Harris and as well as to experimental results. The transient motion of rolling elements and skidding is then investigated during acceleration using the new model.

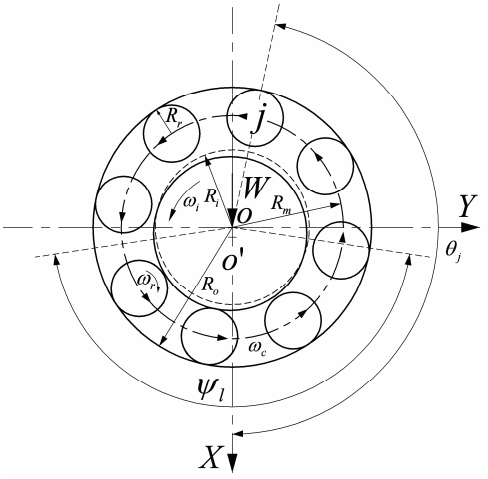

Fig. 1. A schematic diagram of a typical rolling element bearing.

The paper is organized as follows. The model to investigate skidding in rolling element bearings during acceleration is presented in Section 2. The model is validated in Section 3. The numerical results for a deep groove ball bearing are analyzed in Section 4. Finally, the paper is then concluded in Section 5.

2. The problem formulation

A schematic diagram of a typical rolling element bearing is shown in Fig. 1. The outer race is fixed in a rigid support and the inner race rotates with the shaft (angular velocity ω_i). A constant vertical radial force (W) acts on the bearing. R_i is inner raceway radius, R_o is outer raceway radius, R_m is pitch radius of bearing, R_r is radius of rolling element, ω_r represents angular velocity of rolling element about its axis, ω_c represents angular velocity of cage, ψ_l represents angle range of load zone, θ_j represents angle position of jth rolling element.

Elastic deformation between races and rolling elements gives a nonlinear force deformation relationship, which is obtained by the Hertzian theory. The Coulomb friction law is used to calculate the friction force and friction coefficient changes along with relative sliding speed.

A model that represents a real rolling element bearing with

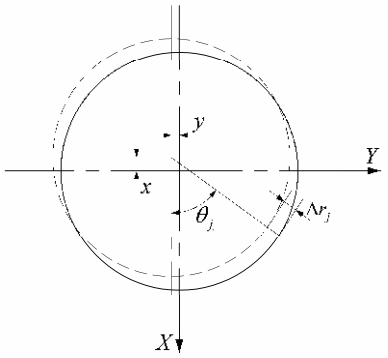

Fig. 2. Inner race displacement.

skidding would be extremely complex. An effective and simplified mathematical model can still be generated if the following assumptions are made.

(1) The rolling elements and the inner and outer races have motions in the plane of the bearing only.

(2) All the bearing components are rigid, resulting in no bending deformation.

(3) We neglect the effect of bearing radial clearance and clearance between rolling elements and the cage pocket.

(4) We neglect the fluid pressure force due to the lubricant.

2.1 Calculation of normal force

According to the Hertzian contact deformation theory, the non-linear relationship between load and deformation is given by [8]

$$N = K\delta^n \tag{1}$$

where n is the load-deformation exponent, n = 3/2 for ball bearings and 10/9 for the roller bearings.

The schematic diagram for determining the deformation is shown in Fig. 2. The terms x and y are the inner race displacements along the X-axis and Y-axis and r_j is the jth rolling element radial displacement. The deformation between inner race and rolling element at the jth rolling element at angle position θ_j is given by

$$\delta_{ij} = [x\cos\theta_j + y\sin\theta_j - r_j]_+ \tag{2}$$

the "+" sign as a subscript in Eq. (2) signifies that the expression within the brackets can't be less than zero, if the expression within the brackets is negative, the deformation is set to zero.

The deformation between the outer race and the jth rolling element at angle position θ_j is given by

$$\delta_{oj} = [r_j]_+ \tag{3}$$

if the expression within the brackets is negative or zero, then the rolling element is not in the load zone and the deformation is set to zero.

The contact force between inner race and the jth rolling element at angle position θ_j can be expressed as

$$N_{ij} = K_i{\delta_{ij}}^n \tag{4}$$

where K_i is the stiffness coefficient between the inner race and the rolling element.

The contact force between outer race and the jth rolling element at angle position θ_j can be expressed as

$$N_{oj} = K_o{\delta_{oj}}^n \tag{5}$$

where K_o is the stiffness coefficient between outer race and rolling element.

If a rolling element runs faster than the cage, the rolling element will contact the front cage pocket and if a rolling element runs slower than the cage, the rolling element will contact the rear cage pocket. Therefore, the contact normal force between the front of the rolling element and the pocket at the jth rolling element can be expressed as

$$N_{c1j} = \begin{cases} K_c[(\psi_j - \psi_c)R_m]^n & (\psi_j - \psi_c)R_m > 0 \\ 0 & else \end{cases} \tag{6}$$

where K_c is the stiffness coefficient between the cage and the rolling element, ψ_j is the rotating angle of the jth rolling element about the bearing axis, and ψ_c is the rotational angle of the cage.

The contact normal force between the rear of the rolling element and the pocket at the jth rolling element can be expressed as

$$N_{c2j} = \begin{cases} K_c[(\psi_c - \psi_j)R_m]^n & (\psi_j - \psi_c)R_m < 0 \\ 0 & else \end{cases}. \tag{7}$$

2.2 Calculation of friction force

The friction force at all contact points is computed as a product of the friction coefficient and the normal force. The friction coefficient at the rolling element-race contact is modeled using a nonlinear friction-slip relationship that is characteristic of most common lubricants [7]. The friction-slip relationship is shown in Fig. 3. The friction coefficient is a function of slip velocity and the relationship can be expressed as follows:

$$u = f(V). \tag{8}$$

Since the slip velocities at the rolling element-cage contact are typically large, a constant friction coefficient is used at the rolling element-cage pocket contact [15].

To determine the friction force between rolling elements

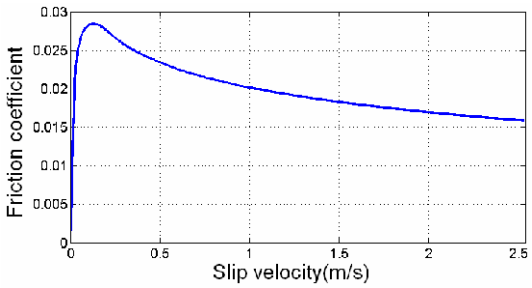

Fig. 3. Friction coefficient is a function of slip velocity [7].

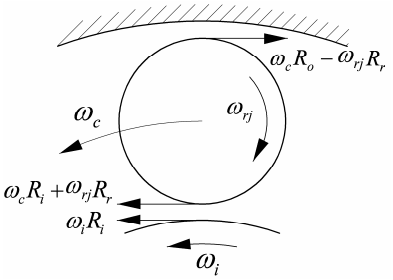

Fig. 4. Surface velocities and slip velocities between rolling elements and races [5].

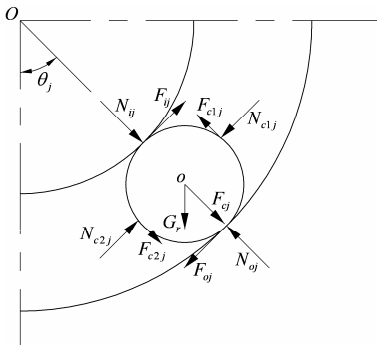

Fig. 5. Forces acting on the jth rolling element.

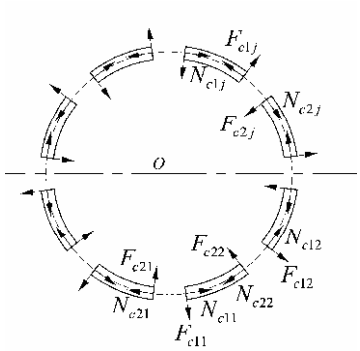

Fig. 6. Forces acting on the cage.

and races, it is first necessary to analyze the slip velocity between the rolling elements and races. Fig. 4 shows the surface velocities and slip velocities between rolling elements and races. The inner race rotates at ω_i radians per second and the outer race is stationary. From Fig. 4, slip velocity between the jth rolling element and the inner race can be expressed as [5]

$$V_{ij} = (\omega_i - \omega_c)R_i - \omega_{rj}R_r \ . \tag{9}$$

Slip velocity between the jth rolling element and the outer race can be expressed as

$$V_{oj} = \omega_c R_o - \omega_{rj}R_r \ . \tag{10}$$

Coulomb friction is used for dry contacts as well as boundary and mixed lubricated contacts. It is often used to describe the friction in mechanical contacts [12]. According to the Coulomb friction law, the friction force between the jth rolling element and the inner race can be determined by

$$F_{ij} = uN_{ij} \ . \tag{11}$$

Friction force between the jth rolling element and the outer race can be expressed as

$$F_{oj} = uN_{oj} \ . \tag{12}$$

The friction force at the front interface between the rolling element and the race pocket at the jth rolling element can be expressed as

$$F_{c1j} = uN_{c1j} \ . \tag{13}$$

The friction force at the rear interface between the rolling element and the pocket at the jth rolling element can be expressed as

$$F_{c2j} = uN_{c2j} \ . \tag{14}$$

2.3 Differential equations of motion

The equations of motion that describe bearing dynamic behavior can be derived from Newton's laws. To derive these equations of motion it is first necessary to analyze the forces acting upon the separate rolling elements, the cage and the inner race.

Forces acting upon the jth rolling element are shown in Fig. 5. In that illustration, N_{ij} and N_{oj} are contact normal forces acting between the jth rolling element and the races. F_{ij} and F_{oj} are friction forces between the jth rolling element and the races. N_{c1j} and N_{c2j} are normal forces at the jth rolling element/pocket contact. F_{c1j} and F_{c2j} are friction forces at the jth rolling element/pocket contact. G_r is the force of gravity acting on the rolling element. F_{cj} is the centrifugal force acting on the jth rolling element due to the cage speed ω_c. Forces acting upon the cage are shown in Fig. 6.

For the jth rolling element, the application of the Newton's second law yields

Table 1. Bearing parameters.

Number of rollers N_b	36
Pitch diameter D_m (mm)	183
Roller diameter D_r (mm)	14
Roller length l_r (mm)	20

$$N_{ij} - N_{oj} - F_{c1j} + F_{c2j} + F_{cj} + G_r \cos\theta_j = m_r \ddot{r}_j \quad (15)$$

$$F_{ij} - F_{oj} - N_{c1j} + N_{c2j} - G_{rj} \sin\theta_j = m_r R_m \ddot{\psi}_j \quad (16)$$

$$(F_{ij} + F_{oj})R_r - (F_{c1j} + F_{c2j})R_r = J_r \dot{\omega}_{rj} \quad (17)$$

where

$$\theta_j = (j-1)\frac{2\pi}{N_b} + \psi_j \quad (18)$$

$$F_{cj} = m_r \dot{\psi}_j^2 R_m \,. \quad (19)$$

Similarly, for the cage:

$$R_m \cdot \sum_{i=1}^{N} (N_{c1j} - N_{c2j}) = J_c \ddot{\psi}_c \quad (20)$$

with

$$\omega_c = \dot{\psi}_c \,. \quad (21)$$

For the inner race:

$$W - \sum_{i=1}^{N} (N_{ij} \cos\theta_j - F_{ij} \sin\theta_j) = m_i \ddot{x} \quad (22)$$

$$-\sum_{i=1}^{N} (N_{ij} \sin\theta_j + F_{ij} \cos\theta_j) = m_i \ddot{y} \,. \quad (23)$$

The system equations of motion are nonlinear ordinary second order differential equations. They can be solved using a fourth-order Runge-Kutta algorithm with fixed time step. The time step for the numerical investigation is chosen to be $\Delta t = 1 \times 10^{-5}$ s.

3. Validations

To ascertain the results of the foregoing analysis, a parametric study was performed on a single row, cylindrical roller bearing having the pertinent dimensions shown in Table 1 [5].

The inner race rotates at a constant speed of 5000 RPM. Fig. 7 shows the comparison of cage speed versus radial load against the Harris model [5] and experimental data. The shape of the curve obtained from the new model closely approximates the curves from the Harris model and the experimental data. This good agreement shows the effectiveness of the proposed model.

Table 2. Bearing parameters of deep groove bearing 6304.

Parameter	Value	Parameter	Value
N_b	7	m_r (kg)	3.50×10^{-3}
R_o (mm)	22.77	J_r (kg·m^2)	3.18×10^{-8}
R_i (mm)	13.24	J_c (kg·m^2)	0.82×10^{-6}
R_m (mm)	18.00	K_i (N/m$^{1.5}$)	3.19×10^{10}
R_r (mm)	4.76	K_o (N/m$^{1.5}$)	3.38×10^{10}
m_i (kg)	0.04	K_c (N/m$^{1.5}$)	6.06×10^{9}

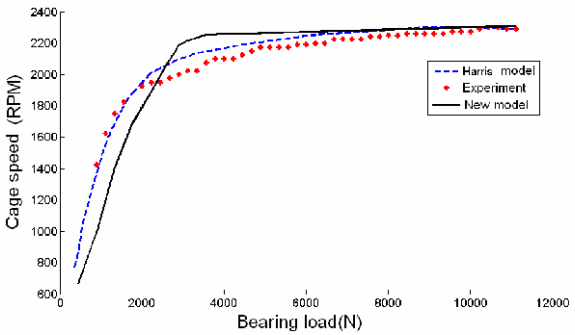

Fig. 7. Comparison of results.

4. Results and discussion

A deep groove ball bearing (NTN 6304) which is widely used in automobile gearbox, is taken as the research object in this paper. The main bearing parameters are listed in Table 2.

Automobile accelerate urgently sometimes and it will causes serious skidding in the rolling element bearing, the angular acceleration of the bearing is very large, it is assumed that the rotational speed of inner race increases from zero to 5000 RPM within one second (angular acceleration 523 rad/s^2). The load applied on the bearing is small generally, three light loads are selected for the simulations, the radial loads acting on the bearing are set to 0.1 N, 1.0 N and 5.0 N, respectively.

4.1 Slip between rolling elements and races

The time-varying slip velocities between rolling elements and the inner race during acceleration are shown in Fig. 8. The slip velocities increase almost exactly linearly with some minor accompanying "steps" due to the contact force between each rolling element and the inner race vanishing when the rolling element moves from the load zone into the non-load zone. When a large radial load is applied on the bearing, the slip velocity increases only in the early stage of the acceleration process and then reduces to zero quickly. This is because the friction force between the rolling elements and the inner race is large enough to drive the rolling element to accelerate to the same speed of the inner race in a short time.

The time-varying slip velocities between rolling elements and the outer race during acceleration are shown in Fig. 9. The slip velocities between the rolling elements and the outer race decrease gradually with some fluctuation. This is because the

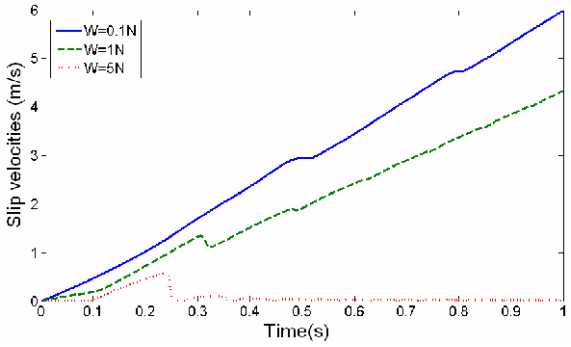

Fig. 8. Slip velocities between rolling elements and the inner race.

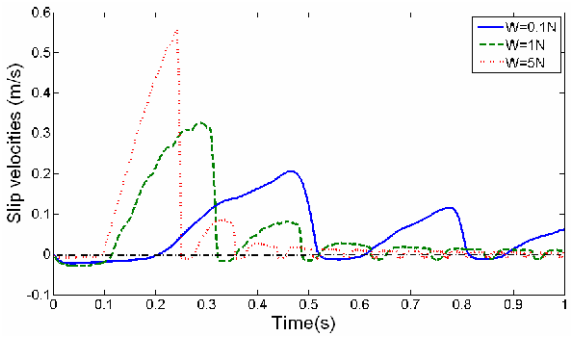

Fig. 9. Slip velocities between a rolling element and the outer race.

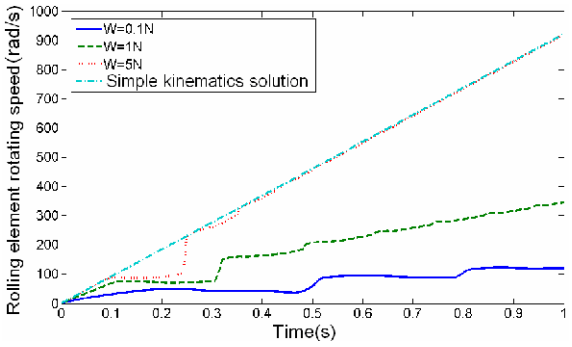

Fig. 10. Rolling element rotating speed as a function of time.

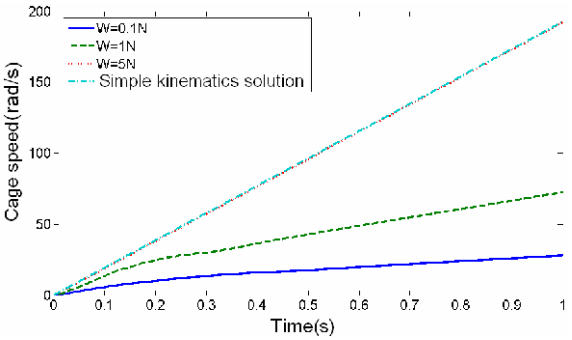

Fig. 11. Cage speed as a function of time.

rolling element acceleration is driven by the friction force between each rolling element and the inner race. When a rolling element is located in the load zone there will be skidding between the rolling element and the outer race because of the resistance of the cage. However, when a rolling element is located in the non-load zone the rolling element is pushed forward by the cage and accelerates, so the skidding direction between the rolling element and the cage will reverse. The rolling element rotational speed and cage speed increase gradually during the acceleration process, so the slip velocities between the rolling element and the outer race decrease gradually. When a large radial load is applied on the bearing, the rolling element rotating speed and the cage speed increase quickly, hence the slip velocity between a rolling element and the outer race drops to near zero quickly.

4.2 Rolling element rotating speed and cage speed

It is assumed in the simple kinematics that there is no slip of rolling elements resulting in the surface velocity of a rolling element being equal to the surface velocity of the race at the point of contact. For a bearing having inner race rotation and a stationary outer race, the rolling element rotating speed ω_{rr} and the cage speed ω_{cr} can be calculated as follows [8]:

$$\omega_{rr} = \frac{1}{2}\omega_i \frac{R_i R_o}{R_r R_m} \tag{24}$$

$$\omega_{cr} = \frac{1}{2}\omega_i \left(1 - \frac{R_r}{R_m}\right). \tag{25}$$

The time-varying rolling element rotating speed during acceleration is shown in Fig. 10. The speed again increases approximately linearly accompanied by "steps". This relationship is a result of the contact force between rolling elements and the inner race, which vanishes when rolling elements move from the load zone into the non-load zone. When a small radial load is applied on the bearing the rolling element rotating speed increases slowly. The tendency for the rolling element rotational speed to increase is reduced at later stage. However, when a large radial load is applied on the bearing, the "steps" in these relationships only exist in the early stage of the acceleration process. After the rolling element rotating speed reaches a modest level, it becomes consistent with the solution of simple kinematics.

The time-varying cage speed during acceleration is shown in Fig. 11. The cage speed increases almost linearly. There are large differences in the cage speeds under different radial loads. The larger the radial load, the larger the angular acceleration. When a large radial load is applied on the bearing, the increasing tendency of the cage speed is basically consistent with the simple kinematics solution.

4.3 Slip ratio

The rolling element slip ratio S_r is defined as follows [11]:

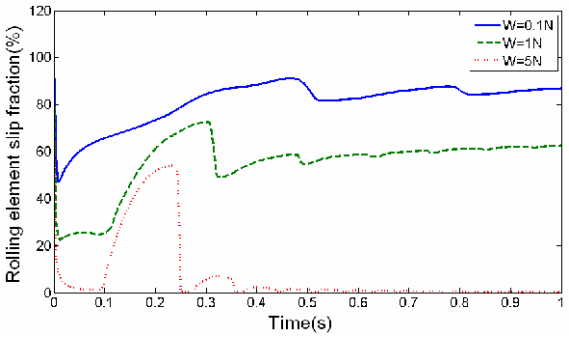

Fig. 12. Rolling element slip ratio.

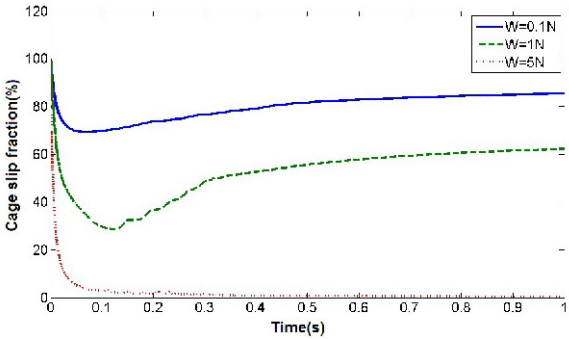

Fig. 13. Cage slip ratio.

$$S_r = (1-\omega_r/\omega_{rr})\times 100\% . \quad (26)$$

The cage slip ratio S_c is defined as follows:

$$S_c = (1-\omega_c/\omega_{cr})\times 100\% \quad (27)$$

where ω_r and ω_c are the results calculated from the proposed model, while ω_{rr} and ω_{cr} are the results from simple kinematics.

The time-varying rolling element slip ratio during acceleration is shown in Fig. 12. This figure shows the rolling element slip ratio varies significantly in the early stages of the acceleration process and then stabilizes gradually as time goes on. This is because the slip ratio decreases rapidly as the rolling element speed increases suddenly from zero in the early stage of the acceleration process and then the rolling element rotational speed decreases because of the friction force, leading to an decrease in the rolling element slip ratio. If the radial load acting upon the bearing is large enough, the rolling element slip ratio will be near zero.

The time-varying cage slip ratio during acceleration is shown in Fig. 13. This figure shows the cage slip ratio decreases in the early stage of the acceleration process and then stabilizes gradually as time goes on. This is because the cage accelerates rapidly caused by the sudden contact forces from rolling elements in the early stage of the acceleration process. As time goes on, the forces from rolling elements stabilize gradually. If the radial load acting upon the bearing is large enough, the cage slip ratio will be near zero.

5. Conclusions

This paper proposes an analytical model to investigate skidding in rolling element bearing during acceleration. The dynamic analysis in this investigation is presented as a design tool for applications where the bearing is subjected to skid due to rotational acceleration of the inner race. The formulation not only estimates the expected wear during skid, but also provides a means to determine the effectiveness of different means employed to eliminate skidding. The following specific conclusions can be stated.

(1) The results from the proposed model agree well with the results from the Harris modal and the experimental data. It is proven that the proposed model is effective.

(2) Rolling element rotating speed increases with some minor variability during constant acceleration of the bearing, while the cage speed increases almost linearly.

(3) The radial load acting on rolling elements has a significant effect on the skidding in the bearing and skidding is most serious during acceleration under light load conditions.

Acknowledgment

This study was financially supported by the National Natural Science Foundation of China under contact no. 51035008.

Nomenclature

ω	: Angular speed, rad/s
W	: Radial load, N
R	: Radius, mm
R_m	: Bearing pitch radius, mm
θ	: Angle position of rolling element, rad
ψ	: Rotational angle of rolling element about the bearing axis, rad
ψ_c	: Rotational angle of the cage, rad
ψ_l	: Load zone, rad
F	: Friction force at rolling element/race, N
F_c	: Centrifugal force, N
F_{c1}	: Friction force at front rolling element/pocket, N
F_{c2}	: Friction force at rear rolling element/pocket, N
n	: Load-deformation exponent
K	: Stiffness coefficient, N/m$^{1.5}$
N_b	: Number of rolling elements
J_r	: Inertia of rolling element, kg·m^2
J_c	: Inertia of the cage, kg·m^2
m	: Mass, kg
N	: Normal force, N
N_{c1}	: Normal force at front rolling element/pocket, N
N_{c2}	: Normal force at rear rolling element/pocket, N
G_r	: Force of gravity, N
δ	: Contact deformation, mm
μ	: Friction coefficient

Subscripts

i : Inner race
o : Outer race
c : Cage
j : Rolling element number
r : Rolling element

References

[1] A. B. Jones, Ball motion and sliding friction in ball bearing, *ASME Trans*., 81 (1959) 1-12.

[2] A. B. Jones, A general theory for elastically constrained ball and roller bearings under arbitrary load and speed conditions, *ASME Trans.,* 82 (1960) 309-320.

[3] T. A. Harris, Ball motion in thrust-load angular contact bearings with coulomb friction, Journal of Lubrication Technology, *Transactions of the ASME,* 95 (1971) 32-38.

[4] T. A. Harris, An analytical model to predict skidding in thrust-loaded, angular-contact ball bearings, Journal of Lubrication Technology, *Transactions of the ASME,* 93 (1971) 17-24.

[5] T. A. Harris, An analytical model to predict skidding in high speed roller bearings, *ASME Trans.,* 9 (1966) 229-241.

[6] C. T. Walters, The dynamics of ball bearings, *Journal of Lubrication Technology,* 93 (1971) 1-10.

[7] P. K. Gupta, Transient ball motion and skid in ball bearings, *Journal of Lubrication Technology* (1975) 261-269.

[8] T. A. Harris and K. MichealN, *Rolling bearing analysis-essential concepts of bearing technology*, 5th Ed. Taylor and Francis; (2007).

[9] F. Hirano, Motion of a ball in angular-contact ball bearing, *ASLE Trans*., 8 (1965) 425-434.

[10] N. T. Liao and L. F. Lin, Ball bearing skidding under radial and axial loads, *Mechanism and Machine Theory,* 37 (2002) 91-113.

[11] A. Selvaraj and R. Marappan, Experimental analysis of factors influencing the cage slip in cylindrical roller bearing, *Inv J Adv Manuf Technol* (2010).

[12] S. Andersson, A. Soderberg and S. Bjorklund, Friction models for sliding dry, boundary and mixed lubricated contacts, *Tribology International*, 40 (2007) 580-587.

[13] E. Laniado-Jacome, J. Meneses-Alonso and V. Diaz-Lopez, A study of sliding between rollers and races in a roller bearing with a numerical model for mechanical event simulations. *Tribology International* (2010).

[14] S. Jain and H. Hunt, A dynamic model to predict the occurrence of skidding in wind-turbine bearings, *9th International Conference on Damage Assessment of Structures* (2011).

[15] N. Ghaisas, C. R. Wassgren and F. Sadeghi, Cage instabilities in cylindrical roller bearing, *Journal of Tribology*, 126 (2004) 681-689.

Wenbing Tu, born in 1983, is currently a Ph.D student of Chongqing University, People's Republic of China. He conducts research in the areas of structural dynamics and numerical simulation, vibration and noise of mechanical system.

Yimin Shao is a full Professor in the State Key Laboratory of Mechanical Transmission at Chongqing University, Chongqing, China. His research interests include machine dynamic analysis, vibration analysis, signal processing and on-line machinery condition monitoring and fault diagnosis system.

Chris K. Mechefske is a full Professor in the Department of Mechanical and Materials Engineering at Queen's University in Kingston, Ontario, Canada. His research interests include vibration based machine condition monitoring and fault diagnostics, maintenance and reliability, machine dynamic analysis, biomechanics of artificial limbs, vibration and noise reduction in and around biomedical equipment. He is a member of the editorial board of the Journal of Condition Monitoring and Diagnostic Engineering Management; Canadian Advisory Council, ISO Technical Committee 108, Sub-Committee 5; American Society of Mechanical Engineers; Canadian Machinery Vibration Association (past president 2003-2005); and the International Institute of Acoustics and Vibration (Director 2007-2009).